

## TRANSIENT MIXED CONVECTION FLOW OF HEAT GENERATING/ABSORBING FLUID DUE TO EXPONENTIALLY DECAYING PRESSURE GRADIENTS IN A VERTICAL POROUS MICROCHANNEL

*A. O. Ajibade and S. I. Toki*

Department of Mathematics, Ahmadu Bello University, Zaria, Nigeria.

### Abstract

*This article considers a theoretical analysis of transient mixed convection flow of heat generating/absorbing fluid due to exponentially decaying pressure gradients in a vertical porous microchannel. The solution of the governing equations is obtained by the Laplace transform technique. However, Riemann-sum approximation approach is used to invert the solution from Laplace domain into time domain. The effects of various flow parameters entering into the problem are discussed with the aid of line graphs. It is interesting to found that rarefaction increase has a decreasing effect on the fluid temperature while it has an increasing effect on velocity.*

**Keywords:** Transient; mixed convection; heat generation/absorption; pressure gradient and microchannel.

Nomenclature			Greek symbols		
$C_p$	Specific heat per constant pressure	$[m^2 s^{-2} K^{-1}]$	$\alpha$	Thermal diffusivity	$[m^2 s^{-1}]$
$Kn$	Knudsen number		$\beta$	Coefficient of thermal expansion	$[K^{-1}]$
$h$	Half channel width	$[m]$	$\beta_v, \beta_t$	Dimensionless variables ratio of specific heat	
Pr	Prandtl number		$\gamma$	Specific heat ratio	
$Gr$	Grashof number		$\lambda$	Mean free path length	$[m]$
$Gre$	Mixed convection parameter		$\rho$	Density	
Re	Reynolds number		$\mu$	Dynamic viscosity	$[Kgm^{-1}s^{-1}]$
$g$	Acceleration due to gravity	$[ms^{-2}]$	$\nu$	Kinematic viscosity	$[m^2 s^{-1}]$
$T$	Temperature of the fluid	$[K]$	$\theta$	Dimensionless temperature	
$T_0$	Ambient temperature	$[K]$	$\sigma_T$	Thermal accommodation coefficient	
$T_1$	Dimensionless temperature at $y = -1$	$[K]$	$\sigma_v$	Tangential momentum accommodation coefficient	
$T_2$	Dimensionless temperature at $y = 1$	$[K]$	$\omega$	Dimensionless frequency	
$B_1, B_2$	Amplitude of oscillatory heating				
$\delta$	Dimensionless heat generating parameter				
$t'$	Dimensional time	$[s]$			
$t$	Dimensionless time				
$k$	Thermal conductivity	$[kgms^{-3}K^{-1}]$			
$u'$	Dimensional velocity	$[ms^{-1}]$			
$u$	Dimensionless velocity				
$u_0$	Reference velocity				
$H$	Suction/injection parameter				
$V_0$	Initial velocity of suction	$[ms^{-1}]$			
$A$	Amplitude of the pressure gradient				
$y'$	Dimensional radial co-ordinate	$[m]$			
$y$	Dimensionless radial co-ordinate				
$Nu$	Nusselt number				
$\tau$	Skin friction				

### 1. INTRODUCTION

Mixed convection flows known as combined forced and free convection flows have long been an important subject in the field of Chemical, Biomedical, Physical, environmental engineering, science, engineering and other related field. They play significant role in

Corresponding Author: Ajibade A.O., Email: aoajibade@abu.edu.ng, Tel: +2348031800282, +2348033246374 (SIT)

*Journal of the Nigerian Association of Mathematical Physics Volume 56, (March - May 2020 Issue), 1 –10*

boundary layers flows, heat exchangers, solar collectors, nuclear reactors and in electronic equipment. Recently, advances in science and technology have promoted a rapid development of different microfluidic devices, as a result of difficulty in making precise measurements, microscale fluid flow and heat transfer modelling were emphasized in modern microfluidic applications such as microelectrochemical cell transport, microheat exchanging, and microchip cooling. These applications have strongly motivated interest in understanding the phenomenological aspects of these small systems and the physical laws governing them. One of the basic steps in understanding these physical aspects is the experimental or theoretical study of flows through a channel of microscale size commonly referred to as microchannels. Several numerical and analytical studies have been conducted in order to provide a deeper understanding of the fluidic behavior within these micro devices. However, no studies have been carried out on transient mixed convection flow of heat generating/absorbing fluid due to exponentially decaying pressure gradient in a vertical micro porous channel.

In [1] transient mixed convective flow of reactive viscous fluid in vertical tube was presented and discovered that, as mixed convection parameter ( $Gr_e$ ) increases the velocity increases in the reverse flow direction. Also as reactant consumption parameter increases the skin friction decreases monotonically while the rate of heat transfer increases monotonically. Looking into [2] transient mixed convection flow of a viscoelastic fluid over a vertical stretching sheet coupled with heat-mass transfer and chemical reaction was studied and discovered that time integration parameter enhances the flow, Viscoelastic parameter and magnetic parameter reduces the thickness of the fluid. While Dufour number increases the temperature field where as the Soret number reduces temperature field. In [3] transient free convection in a vertical channel with variable temperature and mass diffusion was the centre of the study and revealed that, velocity and temperature fields decrease with an increase in radiation parameter. We noticed that [4] employed Laplace transform technique for transient laminar MHD free convective heat transfer past a vertical plate with heat generation and revealed that heat generation parameter is observed to cause a decrease in the skin friction but an increase in the Nusselt number as the heat generation parameter increases. While [5] presented a semi-analytical approach of transient free convective flow in an annular porous medium and observed that velocity and temperature increases with time and finally attains its steady state status.

In [6] mixed convection boundary layer flow towards a vertical plate with a convective surface boundary condition was studied, the result obtained indicate that dual solution exist for the opposing flow, whereas for the assisting flow, the solution is unique. Mixed convection boundary layers in the stagnation-point flow toward a stretching vertical sheet was studied in [7] and discovered that, both the skin friction coefficient and the local Nusselt number decrease as the buoyancy parameter increases, but both increase as ( $\beta_r$ ) increases. Steady periodic regime of mixed convection in a vertical tube filled with porous material having time-periodic boundary condition was discuss in [8] and revealed that velocity is maximum at two different locations in the flow domain, one near the surface of the tube and another at the axis of the tube. We saw the presentation of the steady periodic regime of role of heat generation/absorption on mixed convection flow in a vertical tube filled with porous having time periodic boundary condition in [9] and discovered that the presence of heat generation parameter is seen to enhance the temperature distribution and this is reflected as increase in the magnitude of the oscillation dimensionless velocity, whereas in the presence of a heat absorption a reversed trend occurs. It is observed in [10] that, the effect of slip and heat generation/absorption on MHD mixed convection flow of a micropolar fluid over a heated stretching surface was studied and revealed that increasing the heat generation parameter leads to a rise in both the velocity and the temperature and a fall in the skin friction coefficient and the local Nusselt number. While [11] studied the effects of thermal dissipation, heat generation/absorption on MHD mixed convection boundary layer flow over a permeable vertical flat plate embedded in an anisotropic porous medium and revealed that improving suction strength decreases both the momentum and boundary layer thickness and in consequence delays the boundary layer separation while injection acts the other way round. In [12] steady periodic regime on impact of heat generation/absorption on MHD mixed convection flow in a vertical tube having time periodic boundary condition was studied and revealed that an increase of the heat generation parameter enhanced the rate of heat transfer, whereas an increase in the heat absorption parameter reduced the rate of heat transfer. Also, [13] presented an exact solution for steady fully developed mixed convection flow in a vertical micro-concentric-annulus with heat generating/absorbing fluid and revealed that increase in heat generation parameter enhanced the temperature and the velocity of the fluid but reduced that rate of heat transfer at the outer surface of the inner cylinder while the reverse trend is observed for heat absorbing fluid.

We discovered in [14] that, MHD couette flow and heat transfer of a dusty fluid with exponentially decaying pressure gradient was studied and revealed that suction velocity has a more apparent effect than magnetic field on the steady state time of the velocity and temperature of the dust particles. Whereas [15] studied pressure gradient and electroosmotic effects on two immiscible fluids in a microchannel between two parallel plates. The results obtained demonstrate the interfacial shear stress tendency to decrease when the interface increases. [16] investigate numerical study of the effects of suction and pressure gradient on an unsteady MHD fluid flow between two parallel plates in a non-Darcy porous medium and discovered that the velocity boundary layer thickness increases with increase in the value of suction parameter.

In [17] natural convection in a vertical microchannel was studied and concluded that the temperature jump condition induced by the effects of rarefaction and fluid wall interaction plays an important role in slip-flow natural convection. It was discovered in [18] that increase in the value of rarefaction parameter leads to enhancement in volume flow rate. Recently, [19] theoretically studied the effect of frequency of fluctuating driving force on velocity slip and temperature jump at the walls in four cases of basic gaseous micro-flow problem. The cases considered are transient couette flow, the pulsating poisseuille flow, the Stoke's second problem flow and transient natural convection flow, it was revealed that when the frequency is small the velocity and temperature profiles are similar to the corresponding classical macro flow profiles at zero frequency. Also, the slip in velocity and the jump in temperature increase as the Knudsen number and or the frequency of the driven force increases. While, [20] uses Laplace transform method to investigate dual-phase-lag and Dufour effects on unsteady double-diffusive convection flow in a vertical microchannel filled with porous material and discovered that, mass flux increases within the channel as the porosity increases while the mean temperature of the fluid can be

simultaneously growing the Duder number and thermal retardation time. In all the works mention above, none considered transient mixed convection flow of heat generation/absorbing fluid due to exponentially decaying pressure gradients in a vertical porous microchannel.

This work is remodeled from [19] to consider the effect of suction/injection, mixed convection, heat generation/absorption and amplitude of pressure gradient. However, transient flows in porous media is useful in soil physics and engineering. This necessitates the present study.

**2. Mathematical Formulation**

The flow considered is fully developed steady mixed convection flow of viscous, incompressible, electrically conduction fluid in a micro-channel formed by two vertical porous plates under the effect of transverse magnetic field as presented in Fig. 1.

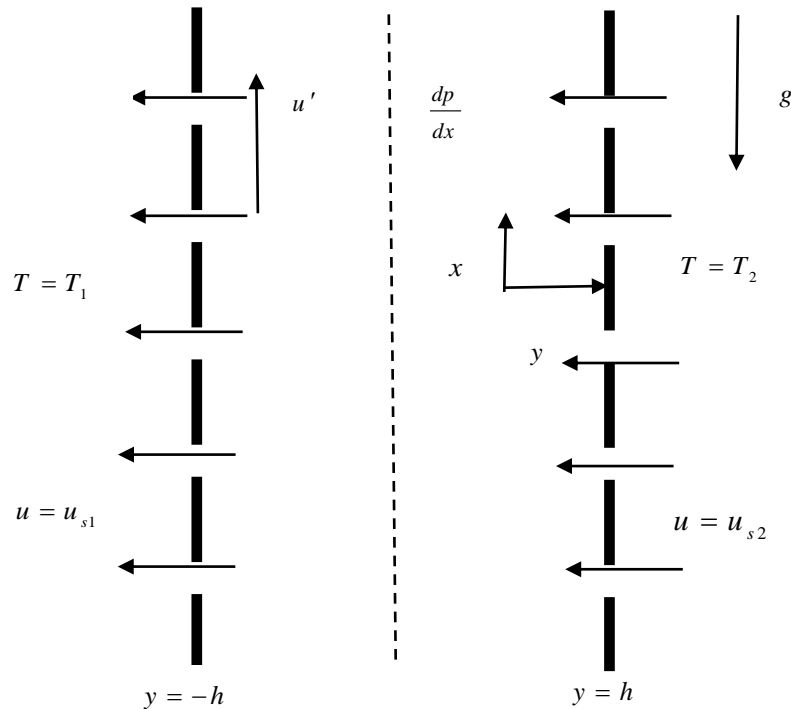


Fig. 1 Schematic diagram of the flow domain

A Cartesian coordinate system with the  $x$ -axis along the plate in the vertically upward direction that is parallel to the gravitational acceleration ( $g$ ) with opposite direction while the  $y$ -axis is orthogonal to the vertical parallel plates. It is assumed that the plate  $y = h$ , fluid is injected into the channel with a constant velocity  $V_0$  and it is sucked off from the system through the plate  $y = -h$  at the same rate. The heat generation/absorption heating is introduced on both walls and due to temperature gradient between the walls and the fluid which resulted in buoyancy effect, mixed convection then sets in.

The governing equations for the flow are

$$\frac{\partial u'}{\partial t'} - V_0 \frac{\partial u'}{\partial y'} = \nu \frac{\partial^2 u'}{\partial y'^2} - \frac{1}{\rho} \frac{dp'}{dx'} + g\beta(T' - T_0) \tag{1}$$

$$\frac{\partial T'}{\partial t'} - V_0 \frac{\partial T'}{\partial y'} = \alpha \frac{\partial^2 T'}{\partial y'^2} + Q_0 \frac{(T' - T_0)}{\rho C \rho} \tag{2}$$

Subject to the initial condition of  $u'(0, y) = T'(0, y)$

And the boundary conditions for  $t' \geq 0$  :

$$u'(t, -h) = \left( \frac{2 - \sigma_v}{\sigma_v} \right) \lambda \frac{\partial u'}{\partial y'} \Big|_{y=-h}, \quad u'(t, h) = - \left( \frac{2 - \sigma_v}{\sigma_v} \right) \lambda \frac{\partial u'}{\partial y'} \Big|_{y=h}$$

$$T'(t, -h) = T_1 + \left( \frac{2 - \sigma_r}{\sigma_r} \right) \frac{\lambda K}{\mu C_p} \frac{\partial T'}{\partial y'} \Big|_{y=-h} \tag{3}$$

$$T'(t, h) = T_2 - \left( \frac{2 - \sigma_r}{\sigma_r} \right) \frac{\lambda K}{\mu C_p} \frac{\partial T'}{\partial y'} \Big|_{y=h}$$

Where  $u_0 = \frac{g\beta h^2(T_1 - T_2)}{\nu}$  is the reference velocity

and using the following dimensional parameters

$$y = \frac{y'}{h}, t = \frac{t'\nu}{h^2}, \theta = \frac{T' - T_0}{T_1 - T_2}, Kn = \frac{\lambda}{h}, B_1 \sin \omega t = \frac{T_1 - T_0}{T_1 - T_2}$$

$$B_2 \sin \omega t = \frac{T_2 - T_0}{T_1 - T_2}, A \exp(-\lambda t) = \frac{-h^2 dp'}{\mu u_0 dx'}, u = \frac{u'}{u_0}, H = \frac{V_0 h}{\nu} \tag{4}$$

$$Pr = \frac{\nu}{\alpha} = \frac{\mu C_p}{K}, Re = \frac{h u_0}{\nu}, \delta = \frac{Q_0 h}{K}, Gr = \frac{g\beta h^3(T_1 - T_2)}{\nu^2}$$

Equations (1), (2) and (3) reduce to dimensionless form as

$$\frac{\partial u}{\partial t} - H \frac{\partial u}{\partial y} = \frac{\partial^2 u}{\partial y^2} + A \exp(-\lambda t) + Gre \theta \tag{5}$$

$$\frac{\partial \theta}{\partial t} - H \frac{\partial \theta}{\partial y} = \frac{1}{Pr} \frac{\partial^2 \theta}{\partial y^2} + \frac{\delta \theta}{Pr} \tag{6}$$

Initial condition  $u(0, y) = 0, \theta(0, y) = 0$

And boundary conditions for  $t \geq 0$

$$u(t, y) = \beta_v Kn \frac{\partial u}{\partial y} \Big|_{y=-1}, u(t, y) = -\beta_t Kn \frac{\partial u}{\partial y} \Big|_{y=1} \tag{7}$$

$$\theta(t, y) = B_1 \exp(-\lambda t) + \beta_t Kn \frac{\partial \theta}{\partial y} \Big|_{y=-1}$$

$$\theta(t, y) = B_2 \exp(-\lambda t) - \beta_t Kn \frac{\partial \theta}{\partial y} \Big|_{y=1}$$

Where  $\beta_v = \left( \frac{2 - \sigma_v}{\sigma_v} \right)$  and  $\beta_t = \left( \frac{2 - \sigma_t}{\sigma_t} \right) \left( \frac{1}{Pr} \right) \frac{2\gamma}{1 + \gamma}$

$A$  is the amplitude of the pressure gradient,  $Gre$  is the mixed convection parameter (which is the ratio of  $Gr$  and  $Re$ ),  $H$  is the dimensionless parameter for suction/injection,  $Pr$  is the Prandtl number and  $\omega$  is the frequency. The physical quantities used in (4) are given in the nomenclature. For the value of  $H = 0, A = 0, \delta = 0$  and  $Gre = 1$  the present problem reduces to the problem investigated by Haddad et al [19]

By introducing the Laplace transform of the dimensionless velocity and temperature equations

$$\bar{u}(s, y) = \int_0^\infty u(t, y) \exp(-st) dt, \bar{\theta}(s, y) = \int_0^\infty \theta(t, y) \exp(-st) dt$$

Where  $s$  is the Laplace parameter and employing the Laplace transform properties equations (5) and (6) subject to the initial condition yield

$$\frac{d^2 \bar{u}}{dy^2} + H \frac{d\bar{u}}{dy} - s\bar{u} = \frac{A}{s + \lambda} - Gre C_1 \exp(m_1 y) - Gre C_2 \exp(m_2 y) \tag{8}$$

$$\frac{d^2 \bar{\theta}}{dy^2} + Pr H \frac{d\bar{\theta}}{dy} - \bar{\theta}(s Pr + \delta) = 0 \tag{9}$$

While the boundary conditions in equation (7) can be transform into the Laplace domain to give

$$\bar{u}(s, y) = \beta_v Kn \frac{\partial \bar{u}}{\partial y} \Big|_{y=-1}, \bar{u}(s, y) = -\beta_t Kn \frac{\partial \bar{u}}{\partial y} \Big|_{y=1}$$

$$\bar{\theta}(s, y) = \frac{B_1}{s + \lambda} + \beta_t Kn \frac{\partial \bar{\theta}}{\partial y} \Big|_{y=-1}, \bar{\theta}(s, y) = \frac{B_2}{s + \lambda} - \beta_t Kn \frac{\partial \bar{\theta}}{\partial y} \Big|_{y=1} \tag{10}$$

The solutions to equations (8) and (9) in the Laplace domain (subject to the boundary condition (10)) are given as

$$\bar{u}(t, y) = C_3 \exp(m_3 y) + C_4 \exp(m_4 y) + K_6 + K_7 \exp(m_1 y) + k_8 \exp(m_2 y) \tag{11}$$

$$\bar{\theta}(t, y) = C_1 \exp(m_1 y) + C_2 \exp(m_2 y) \tag{12}$$

Where  $C_1, C_2, C_3, C_4, k_1, k_2, k_3, k_4, k_5, k_6, k_7, k_8, m_1, m_2, m_3, m_4$  are given in the Appendix.

Expression for the Skin friction and Nusselt number in the microchannel is obtain as follows

*Skin friction*

The skin friction on the surface of the boundary plate is obtained by taking the derivative of the velocity and evaluating it on the boundaries to get

$$\bar{\tau}_0 = \left. \frac{d\bar{u}}{dy} \right|_{y=-1} = m_3 C_3 \exp(-m_3) + m_4 C_4 \exp(-m_4) + m_1 K_7 \exp(m_1) + m_2 K_8 \exp(-m_2) \tag{13}$$

$$\bar{\tau}_1 = \left. \frac{d\bar{u}}{dy} \right|_{y=1} = m_3 C_3 \exp(m_3) + m_4 C_4 \exp(m_4) + m_1 K_7 \exp(m_1) + m_2 K_8 \exp(m_2) \tag{14}$$

*Nusselt Number*

The rate of heat transfer from the boundary plates to the fluid is another interesting phenomenon that is investigated. To investigate this, the derivative of temperature is evaluated on the boundary of the channel so that

$$\bar{N}u_0 = \left. \frac{d\bar{\theta}}{dy} \right|_{y=-1} = m_1 C_1 \exp(-m_1) + m_2 C_2 \exp(-m_2) \tag{15}$$

$$\bar{N}u_1 = \left. \frac{d\bar{\theta}}{dy} \right|_{y=1} = m_1 C_1 \exp(m_1) + m_2 C_2 \exp(m_2) \tag{16}$$

Equations (11) to (16) are to be inverted in order to determine the velocity and temperature in the time domain. Because these equations are difficult to invert in closed form, then we use a numerical procedure that is based on the Riemann-sum approximation Ajibade [20]. In this method, functions in the Laplace domain equation s can be inverted to the time domain t as follows

$$u(t, y) = \frac{e^{\epsilon t}}{t} \left( \frac{1}{2} \bar{u}(y, \epsilon) + \text{Re} \sum_{k=1}^N (-1)^k \bar{u} \left( y, \epsilon + \frac{ik\pi}{t} \right) \right) \tag{17}$$

$$\theta(t, y) = \frac{e^{\epsilon t}}{t} \left( \frac{1}{2} \bar{\theta}(y, \epsilon) + \text{Re} \sum_{k=1}^N (-1)^k \bar{\theta} \left( y, \epsilon + \frac{ik\pi}{t} \right) \right) \tag{18}$$

Where  $\text{Re}$  refers to the ‘‘real part of’’ and  $\sqrt{-1}$  is the imaginary number,  $N$  is the number of terms used in the Riemann-sum approximation and  $\epsilon$  is the real part of the Bromwich contour that is used in inverting Laplace transforms. The Riemann-sum approximation for the Laplace inversion involves a single summation for the numerical process. Its accuracy depends on the value of  $\epsilon$  and the truncation error dictated by  $N$ . The value  $\epsilon$  must be selected so that the Bromwich contour encloses all the branch points. For faster convergence, however, numerous numerical experiments have shown that a value satisfying the relation  $\epsilon t \cong 4.7$  Ajibade [20] gives the most satisfactory results. Hence, the appropriate value of  $\epsilon$  for faster convergence depends on the instant of time ( $t$ ) at which the lagging phenomenon is studied. The criterion shown by  $\epsilon t \cong 4.7$  is independent of  $t$ . The number  $N$  of terms used in the Riemann-sum is determined. Thus, a prescribed threshold for the accumulated partial sum is satisfied at given values of  $\epsilon$ ,  $y$  and  $t$ .

**3. RESULTS ANDDISCUSSION.**

The present study investigate the interactive effects of Knudsen number ( $Kn$ ), mixed convection ( $Gre$ ), suction/injection ( $H$ ), Prandtl number ( $Pr$ ), heat generating/absorbing ( $\delta$ ), amplitude of oscillatory heating ( $B_1, B_2$ ), rate of decay of the pressure gradient ( $\lambda$ ), time ( $t$ ), and amplitude of the pressure gradient ( $A$ ).

Fig. 2a and b shows the effects of Knudsen number parameter ( $Kn$ ) on both temperature and velocity profile in the microchannel. It is clear that an increase in rarefaction leads to an increase in temperature jump which leads to a decrease in the effect of applied boundary temperature and a corresponding decrease in the fluid temperature within the microchannel. Also, an increase in the rarefaction decreases the retarding effects of the microchannel boundary thereby resulting to increase in fluid velocity. This is physically true since increase in Knudsen number increases the mean free path of the molecules, and this lead to decrease in retarding effect of the microchnnel walls. Figure 3a and b shows the effect of suction/injection on velocity and temperature profiles. It is visible from fig. 3a that the temperature decrease monotonically near the wall  $y = -1$  and increases monotonically near the wall  $y = 1$  with the increase in suction through the plate  $y = -1$ . This is true physically since an increase in suction causes a slight decline in momentum boundary layer thickness. In fig 3b, for negative values of  $H$  (injection through  $y = -1$ ), fluid velocity decreases near the wall  $y = -1$  while it increases about the other wall. The reverse of this phenomena is observed for positive values of  $H$  (suction). This is true because increase in suction weakens the thermal boundary layer of the fluid force while injection thickens the thermal boundary layer. Fig 4 shows that an increase in mixed convection parameter ( $Gre$ ) enhances the fluid flow velocity while a decrease in  $Gre$  decreases the fluid flow velocity due to cooling. Physically, the thermal  $Gre$  signifies the relative effect of the thermal buoyancy force to the viscous hydrodynamic fore in the boundary layer, as expected there is a rise in the velocity due to enhancement of thermal buoyancy force. This is physically true since increase in  $Gre$  amplifies the fluid buoyancy and strengthens convection current through the cahnel. Fig 5aand 5b shows the temperature and velocity profile for different values of the Prandtl number ( $Pr$ ), clearly thermal diffusivity dominates indicating heat conduction is more significant compared to convection. For large value of  $Pr$  the figure reveals a decrease in temperature showing that the heat diffuses slowly compared to velocity (momentum) this means that for liquid metals (with low  $Pr$ ), the thickness of thermal boundary layer is much bigger than velocity boundary layer. Fig. 5b shows that a growing  $Pr$  increases the velocity flow of the microchannel. This is a clear evidence of decrease in temperature with growing  $Pr$  which weakens convection currents within the channel so that fluid velocity decrease.

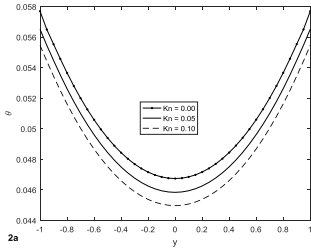


Fig. 2a. Temperature Profile for different values of  $Kn$  [ $H = 0.5, Pr = 0.044, A = 0.1, \delta = 0.5, B_2 = 0.1, t = 0.5, B_1 = 0.1, \lambda = 1.1$ ]

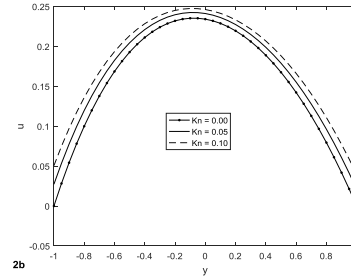


Fig. 2b. Velocity Profile for different values of time  $Kn$  [ $H = 0.5, Pr = 0.044, A = 0.1, \delta = 0.5, B_2 = 0.1, t = 0.5, B_1 = 0.1, \lambda = 1.1$ ]

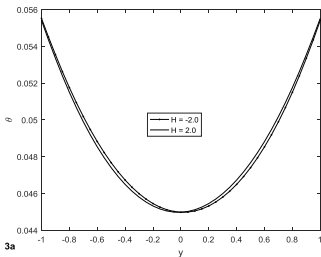


Fig. 3a. Temperature Profile for different values of suction/injection parameter  $H$  [ $B_1 = 0.5, Pr = 0.044, A = 0.1, \delta = 0.5, B_2 = 0.1, t = 0.5, Kn = 0.1, \lambda = 1.1$ ]

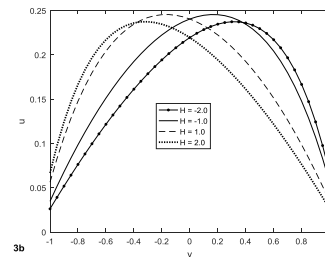


Fig. 3b. Velocity Profile for different values of suction/injection parameter  $H$ , [ $B_1 = 0.1, Pr = 0.044, A = 0.1, \delta = 0.5, B_2 = 0.1, t = 0.5, Kn = 0.1, \lambda = 1.1$ ]

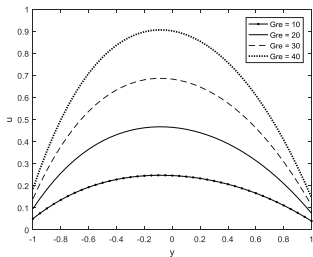


Fig. 4. Velocity Profile for different values of mixed convection parameter  $Gre$  [ $H = 0.5, Pr = 0.044, A = 0.1, \delta = 0.5, B_2 = 0.1, t = 0.5, Kn = 0.1, \lambda = 1.1$ ]

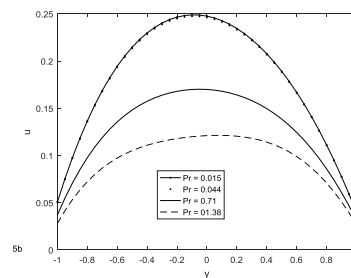


Fig. 5b. Velocity Profile for different values of Prandtl number  $Pr$  [ $H = 0.5, B_1 = 0.1, A = 0.1, \delta = 0.5, B_2 = 0.1, t = 0.5, Kn = 0.1, \lambda = 1.1$ ]

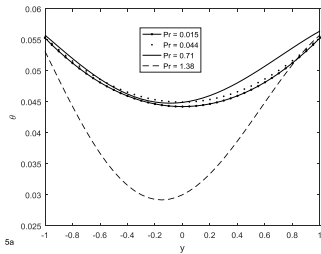


Fig. 5a. Temperature Profile for different values of Prandtl number  $Pr$  [ $H = 0.5, B_1 = 0.1, A = 0.1, \delta = 0.5, B_2 = 0.1, t = 0.5, Kn = 0.1, \lambda = 1.1$ ]

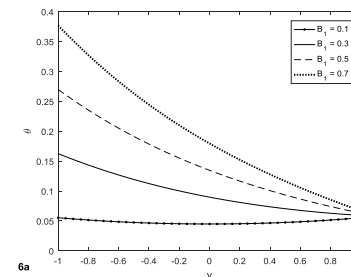


Fig. 6a. Temperature Profile for different values of  $B_1$  [ $H = 0.5, Pr = 0.044, A = 0.1, \delta = 0.5, B_2 = 0.1, t = 0.5, Kn = 0.1, \lambda = 1.1$ ]

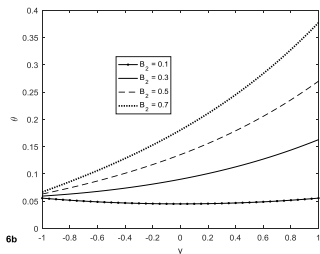


Fig. 6b. Temperature Profile for different values of  $B_2$   
 [  $H = 0.5, Pr = 0.044, A = 0.1, \delta = 0.5,$   
 $B_1 = 0.1, t = 0.5, Kn = 0.1, \lambda = 1.1$  ]

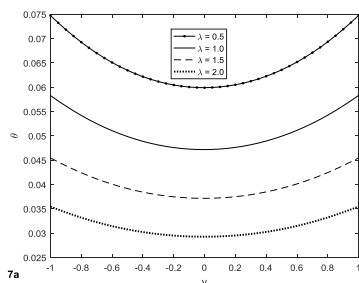


Fig. 7a. Temperature Profile for different values of rate of decay of the pressure gradient parameter  $\lambda$   
 [  $H = 0.5, Pr = 0.044, A = 0.1, \delta = 0.5,$   
 $B_2 = 0.1, t = 0.5, Kn = 0.1, B_1 = 0.1$  ]

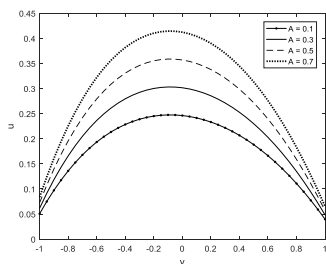


Fig. 9. Velocity Profile for different values of amplitude of the pressure gradient  $A,$   
 [  $H = 0.5, Pr = 0.044, B_1 = 0.1, \delta = 0.5,$   
 $B_2 = 0.1, t = 0.5, Kn = 0.1, \lambda = 1.1$  ]

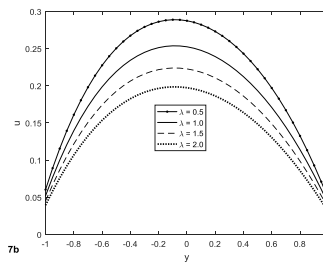


Fig. 7b. Velocity Profile for different values of rate of decay of the pressure gradient parameter  $\lambda$   
 [  $H = 0.5, Pr = 0.044, A = 0.1, \delta = 0.5,$   
 $B_2 = 0.1, t = 0.5, Kn = 0.1, B_1 = 0.1$  ]

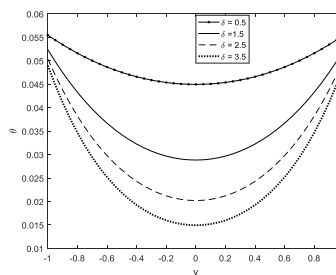


Fig. 8. Temperature Profile for different values of heat generating/absorbing parameter  $\delta$   
 [  $H = 0.5, Pr = 0.044, A = 0.1, B_1 = 0.1,$   
 $B_2 = 0.1, t = 0.5, Kn = 0.1$  ]

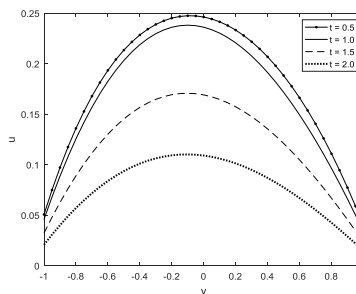


Fig. 10. Velocity Profile for different values of time  $t$   
 [  $H = 0.5, Pr = 0.044, A = 0.1, \delta = 0.5,$   
 $B_2 = 0.1, B_1 = 0.1, Kn = 0.1, \lambda = 1.1$  ]

Fig 6a and 6b captured the temperature profiles for different values of amplitude of time dependent heating ( $B_1, B_2$ ). An increase in the amplitude of thermal input lead to an increase in temperature of the microchannel wall. This is true, due to increase in the volume of the thermal input caused by growing the amplitude of heat input. The resultant effect of the amplitude change is seen to have the maximal effect on the plate whose amplitude was increased while the effect decreases inward towards the other microchannel plate. Fig 7a and 7b shows temperature and velocity profile for different values of rate of decay of the pressure gradient parameter ( $\lambda$ ). This is due to the physical fact that an increase in  $\lambda$  constitutes an overall decrease in the applied temperature on both boundaries due to exponential decay temperature with growing  $\lambda$  therefore an increase in  $\lambda$  leads to a decrease in the temperature profile in the microchannel. In figure 7b however an increase in  $\lambda$  leads to a slight decrease in the velocity of the fluid in the microchannel. This is caused by the combined effect temperature decrease due to increase in  $\lambda$  exponential decay in the pressure gradient so that the mixed convection becomes weakened within the channel and decrease in the fluid velocity. Fig 8 illustrate the influence of the dimensionless heat generating/absorbing coefficient  $\delta$  on the fluid temperature profile. An increase in  $\delta$  leads to a decrease in the temperature profile causing the thermal boundary to become thinner with increasing heat absorption. Fig 9 shows that an increase in amplitude of the pressure gradient ( $A$ ) leads to an increase in the fluid velocity profile. Fig 10 depicts the velocity profile for different values of time ( $t$ ). An increase in  $t$  leads to a decrease in the fluid velocity profile. This is due to the fact that the thermal inputs on both boundary as well as the pressure gradient are exponentially decaying with growing time. This causes a decrease in fluid temperature which results to weakening of the convection current. At the same time, a decrease in the pressure, coupled with a weakened convection current lead to a decrease in velocity as time increases.

The figure further shows a decrease in the boundary slip as time increases

**TABLE 1:** The effect of different flow parameters on the rate of heat transfer (Nusselt number) when  $t = 0.5$

	$(B_1, B_2)$	$H = 0.1, Kn = 0.01$		$H = 0.1, Kn = 0.1$		$H = 0.5, Kn = 0.1$	
		$N_{u0}$	$N_{u1}$	$N_{u0}$	$N_{u1}$	$N_{u0}$	$N_{u1}$
Pr = 0.044	(0.1,0.1)	0.023459	0.023410	0.017795	0.017752	0.017881	0.017666
	(0.1,0.2)	0.005696	0.064427	0.002201	0.050961	0.002012	0.050517
	(0.2,0.2)	0.046917	0.046820	0.035590	0.035504	0.035762	0.035331
Pr = 0.71	(0.1,0.1)	0.006870	0.006260	0.006116	0.005201	0.007714	0.003240
	(0.1,0.2)	0.013623	0.030299	0.010002	0.024385	0.013404	0.016863
	(0.2,0.2)	0.013740	0.012519	0.012232	0.010401	0.015427	0.006481

**TABLE 2:** The effect of different flow parameters on the skin friction when  $t = 0.5$

	$(B_1, B_2)$	$H = 0.1, Kn = 0.01, Pr = 0.044$		$H = 0.1, Kn = 0.01, Pr = 0.71$		$H = 0.5, Kn = 0.1, Pr = 0.71$	
		$\tau_0$	$\tau_1$	$\tau_0$	$\tau_1$	$\tau_0$	$\tau_1$
A = 0.1	(0.1,0.1)	0.458189	0.431808	0.375292	0.357923	0.313928	0.303198
	(0.1,0.2)	0.580278	0.708200	0.453832	0.604555	0.375768	0.511968
	(0.2,0.2)	0.868496	0.818598	0.702702	0.670829	0.583440	0.564280
A = 0.5	(0.1,0.1)	0.649721	0.611875	0.566824	0.537991	0.491592	0.471664
	(0.1,0.2)	0.771810	0.888268	0.645364	0.784623	0.553432	0.680434
	(0.2,0.2)	1.060028	0.998666	0.894233	0.850897	0.761104	0.732746

Table 1 shows the rate of heat transfer on the surface of the boundaries of the microchannel for some selected flow parameters. It is clear that heat transfer rate decrease on both boundaries in the presence of an increasing rarefaction. This is physically true because an increase in  $Kn$  decreases the fluid-wall interaction which actually is a major barrier in the heat transfer between the plates and the fluid. The table also, reveals an increase in heat transfer on the plate  $y = -1$  as suction is increase on the same plate while heat transfer decreases on the plate with injection through it. Increasing the amplitudes of the periodic thermal input cause the boundary temperature to increase causing a corresponding increase in the temperature difference between the channel plates and the adjacent fluid increase in the rate of heat transfer on the boundaries of the microchannel. Finally, decreasing the thermal diffusivity of the fluid causes a delay in growing the fluid temperature so that the temperature gradient increased between the fluid and the plates. That accounts for increase in Nusselt number in case of air as compared to mercury.

The numerical values of the skin friction for some selected flow parameters were captured in table 2. Increasing Prandtl number as well as the rarefaction parameter leads to a decrease in the skin friction while, an increasing the amplitude of the oscillating heating and amplitude of the pressure gradient leads to an increase in the skin friction. The table further shows that an increase in the volume of the thermal input on the boundaries of the microchannel constitute an increase in the skin friction on the surface of both plates of the microchannel.



4. Conclusion

Analytical solution has been obtain for transient mixed convection flow of heat generating/absorbing fluid due to exponentially decaying pressure gradient in a vertical porous microchannel. The governing equations were non dimensionalised and solved using Laplace transform method. From the analysis of the present problem, the following conclusions are drawn

1. An increase in fluid rarefaction causes a decrease in temperature while it has an increasing effect on fluid velocity.
2. Exponential decay of thermal input causes a decrease in fluid temperature while exponential decay of pressure gradient results in decrease in fluid velocity.
3. A decrease in thermal diffusivity of fluid leads to a corresponding decrease in the rate of heat transfer from microchannel plates to the fluid.

Appendix

$$m_1 = \frac{-Pr H + \sqrt{Pr^2 H^2 + 4(S Pr - \delta)}}{2}$$

$$m_2 = \frac{-Pr H - \sqrt{Pr^2 H^2 + 4(S Pr - \delta)}}{2}$$

$$C_1 = K_3 \left( \frac{B_1 K_5 - B_2 K_2}{K_1 K_5 - K_2 K_4} \right)$$

$$C_2 = K_3 \left( \frac{B_1 K_4 - B_2 K_1}{K_2 K_4 - K_1 K_5} \right)$$

$$K_1 = \exp(-m_1) - \beta t K n m_1 \exp(-m_1)$$

$$K_2 = \exp(-m_2) - \beta t K n m_2 \exp(-m_2)$$

$$K_3 = \left( \frac{1}{S + \lambda} \right), K_4 = \exp(m_1) + \beta t K n m_1 \exp(m_1)$$

$$K_5 = \exp(m_2) + \beta t K n m_2 \exp(m_2)$$

$$K_6 = \left( \frac{-A}{S(S + \lambda)} \right)$$

$$C_3 = \left( \frac{K_9 K_{14} - K_{11} K_{12}}{K_{10} K_{14} - K_{11} K_{13}} \right)$$

$$C_4 = \left( \frac{K_9 K_{13} - K_{10} K_{12}}{K_{11} K_{13} - K_{10} K_{14}} \right)$$

$$m_3 = \frac{-H + \sqrt{H^2 + 4S}}{2}$$

$$m_4 = \frac{-H - \sqrt{H^2 + 4S}}{2}$$

$$K_7 = \frac{-GrC_1}{Re(m_1^2 + Hm_1 - S)}$$

$$K_8 = \frac{-GrC_2}{Re(m_2^2 + Hm_2 - S)}$$

$$K_9 = \beta v K n (K_7 m_1 \exp(-m_1) + K_8 m_2 \exp(-m_2)) - K_6 - K_7 \exp(-m_1) - K_8 \exp(-m_2)$$

$$K_{10} = \exp(-m_3) - \beta v K n m_3 \exp(-m_3), K_{14} = \exp(m_4) + \beta v K n m_4 \exp(m_4)$$

$$K_{11} = \exp(-m_4) - \beta v K n m_4 \exp(-m_4), K_{13} = \exp(m_3) + \beta v K n m_3 \exp(m_3),$$

$$K_{12} = -\beta v K n (K_7 m_1 \exp(m_1) + K_8 m_2 \exp(m_2)) - K_6 - K_7 \exp(m_1) - K_8 \exp(m_2)$$

5. Reference.

- [1] Jha B. K, Ahmad K. S., and Ajibade A. O., (2013), Transient Mixed Convection Flow of Reactive Viscous Fluid in Vertical Tube, Afr. Mat. DOI 10.1007/s13370-013-0160-8
- [2] Priyadarsan K. P., Panda S., Nayak A., and Acharya M. R., (2015), Transient Mixed Convection Flow of a Viscoelastic Fluid Over a Vertical Stretching Sheet Coupled with Heat-Mass Transfer and Chemical Reaction. American Journal of Fluid Dynamics 5(3), 76-86
- [3] Mandal H. K., Das S., and Jana R. N., (2014), Transient Free Convection in a Vertical Channel with Variable Temperature and Mass Diffusion. Chemical and process engineering research 23, 2224-7467
- [4] Olisa J. D., (2017), Transient Laminar MHD Free Convective Heat Transfer Past a Vertical Plate with Heat Generation. The International Journal of Engineering and Science 6 (4), 08-13.

- [5] Jha B. K., and Yusuf T. S., (2016), Transient Free Convective Flow in an Annular Porous Medium: A Semi-Analytical Approach, Engineering Science Technology., International Journal, <http://dx.doi.org/10.1016/j.jestch.2016.09.022>
- [6] Amani F., and Ishak A., (2012), Mixed Convection Boundary Layer Flow Towards a Vertical Plate with a Convective Surface Boundary Condition. Hindawi Publication Corporation, Mathematical Problems in Engineering **2012** (11), 453457
- [7] Ishak A., Nazar R., and Pop I., (2006), Mixed Convection Boundary Layers in The Stagnation-Point Flow Toward a Stretching Vertical Sheet. Meccanica **2006**(41), 509-518
- [8] Jha B. K., Ajibade A. O., and Daramola D., (2015), Mixed Convection in a Vertical tube Filled with Porous Material Having Time-Periodic Boundary Condition: Steady Periodic Regime. Afri. Mat. **2015** (26) 529 - 543
- [9] Jha B. K., Daramola D., Ajibade A. O. (2016), Role Heat Generation/Absorption on Mixed Convection Flow in a Vertical Tube Filled With Porous Material Having Time-Periodic Boundary Condition: Steady Periodic Regime, Transport in Porous Media, **111** (3) 681 - 699
- [10] Mahmoud M., and Waheed S., (2010), Effects of Slip and Heat Generation/Absorption on MHD Mixed Convection Flow of a Micropolar Fluid Over a Heated Stretching Surface. Hindawi Publishing Corporation, Math. Prob. in Eng., **2010** (20), 579162
- [11] Adeniyi A., and Aroloye S. J., (2015), Effects of Thermal Dissipation, Heat Generation/Absorption on MHD Mixed Convection Boundary Layer Flow Over a Permeable Vertical Flat Plate Embedded in an Anisotropic Porous Medium. Gen. Math. Notes, **30** (2), 31-53
- [12] Jha B. K., and Aina B., (2016), Impact of Heat Generation/Absorption on MHD Mixed Convection Flow in a Vertical Tube Having Periodic Boundary Condition: Steady-Periodic Regime. Heat Pipe Science and Technology, **7**(1-2) 123-147
- [13] Jha B. K., Oni M. O., and Aina B., (2016), Steady Fully Developed Mixed Convection Flow in a Vertical Micro-Concentric-Annulus with Heat Generation/Absorption Fluid: An Exact Solution, Ain Shams Eng. J, <http://dx.doi.org/10.1016/j.asej.2016.08.005>
- [14] Attia H. A., Al-kaisy A. M. A., and Ewis K. M., (2011), MHD Couette Flow and Heat Transfer of a Dusty Fluid With Exponentially Decaying Pressure Gradient. Tamkang Journal of Sci. and Eng., **14**(2) 91-96
- [15] Ngoma G. D., and Erchiqui F., (2005), Pressure Gradient and Electroosmotic Effects on two Immiscible Fluids in a Microchannel between Two Parallel Plates, J. Micromechanics and Microengineering **16** (2006) 83-91
- [16] Kalai B. S., (2017), Numerical Study of The Effects of Suction and Pressure Gradient on Unsteady MHD Fluid Flow between two Parallel Plates in a Non-Darcy Porous Medium, Asian Research Journal of Mathematics **3**(4), 1-14
- [17] Chen C. K and Weng H. C (2005), Natural Convection in a Vertical Microchannel. Journal of heat transfer, **127** (9), 1053-1056
- [18] Jha B. K., Malgwi P. B., and Aina B., (2017), Hall Effects on MHD Natural Convection Flow in a Vertical Microchannel, Alexandria Eng. J, <http://dx.doi.org/10.1016/j.aej.2017.01.038>
- [19] Haddad O. M., Al-Nimr M. A., Abuzaid M. M., and Irbid J., (2005), The Effect of Frequency of Fluctuating Driving Force on Basic Gaseous Micro-Flows, Acta Mechanical **179** (2005), 249-259
- [20] Ajibade A. O., (2014), Dual-phase-lag and Dufour effects on unsteady double-diffusive convection flow in a vertical microchannel filled with porous material, Journal of Process Mechanical Engineering. **228**(4), 272-285.